Accepted Manuscript

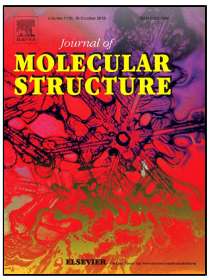

XRD and ATR/FTIR investigations of various montmorillonite clays modified by monocationic and dicationic imidazolium ionic liquids

A. Ahmed, Y. Chaker, El H. Belarbi, O. Abbas, J.N. Chotard, H.B. Abassi, A. Nguyen Van Nhien, M. El Hadri, S. Bresson

PII:	S0022-2860(18)30858-5
DOI:	10.1016/j.molstruc.2018.07.039
Reference:	MOLSTR 25444
To appear in:	*Journal of Molecular Structure*
Received Date:	30 April 2018
Accepted Date:	10 July 2018

Please cite this article as: A. Ahmed, Y. Chaker, El H. Belarbi, O. Abbas, J.N. Chotard, H.B. Abassi, A.Nguyen Van Nhien, M. El Hadri, S. Bresson, XRD and ATR/FTIR investigations of various montmorillonite clays modified by monocationic and dicationic imidazolium ionic liquids, *Journal of Molecular Structure* (2018), doi: 10.1016/j.molstruc.2018.07.039

graphical abstract

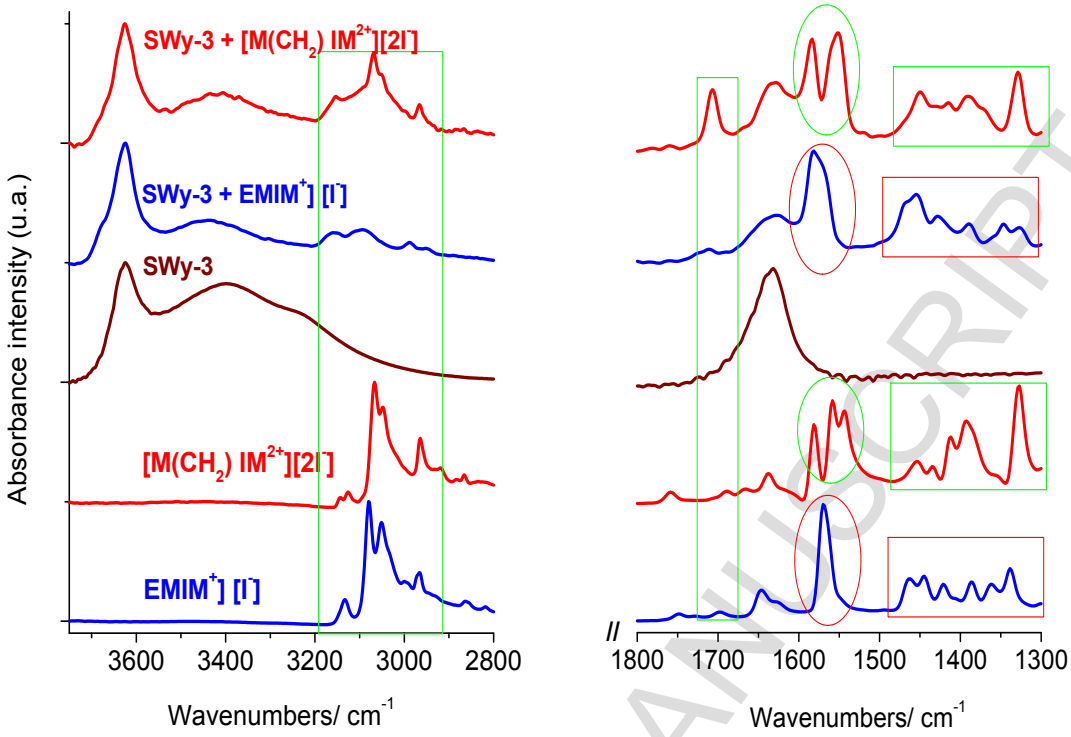

XRD and ATR/FTIR investigations of various montmorillonite clays modified by monocationic and dicationic imidazolium ionic liquids

A. Ahmed[1], Y. Chaker[2], El H. Belarbi[2], O. Abbas[3], J.N. Chotard[4], H. B. Abassi[5], A. Nguyen Van Nhien[5], M. El Hadri[6], S. Bresson*[1]

[1] *Laboratoire de Physique des Systèmes Complexes, Université Picardie Jules Verne, Amiens, France*
[2] *Laboratoire Synthèse et Catalyse, Ibn Khaldoun University, Tiaret, Algeria*
[3] *Walloon Agricultural Research Centre (CRA-W), Valorisation of Agricultural Products, Department, Food and Feed Quality Unit (U15), 'Henseval Building', Chaussée de Namur 24, 5030 Gembloux, Belgium*
[4] *Laboratoire de Réactivité de Chimie du Solide, Université Picardie Jules Verne, 33 rue S^t Leu 80039 Amiens cedex, France*
[5] *Laboratoire de Glycochimie, des Antimicrobiens et des Agroressources CNRS FRE 3517, Institut de Chimie de Picardie CNRS FR 3085, Université Picardie Jules Verne, 33 rue St Leu 80039 Amiens cedex, France*
[6] *Laboratoire de Physique de la Matière Condensée, Université Abdelmalek Essaâdi, Tétouan, Maroc*

ABSRACT

Three different montmorillonites (Mts) labeled K10, KSF and SWy-3 were analyzed by X-ray diffraction and ATR/FTIR spectroscopy. The XRD results enabled validation of the purification process of the studied clays. In the spectral regions 3800-2600 and 1800-1300 cm^{-1}, the study of different intensity ratios of peaks assigned to the O-H bending and stretching modes displayed the specific vibrational behavior of SWy-3 which is certainly influenced by a greater proportion of Na^+ in its structure. Before analyzing the clays modified by ionic liquids, we characterized two imidazolium based ionic liquids (ILs) with anion I^-: [$EMIM^+$] [I^-] monocationic ionic liquid and [$M(CH_2)$ IM^{2+}] [$2I^-$] dicationic ionic liquid. The passage from [$EMIM^+$] [I^-] to [$M(CH_2)$ IM^{2+}] [$2I^-$] reveals significant vibrational changes through various modes: ν(N-H), rings ν(C=C), rings ν(C=N), ν(CH_2(N)), ν(CH_3(N)) in addition to anion interaction modes. When purified, these ionic liquids modify clays, the XRD analysis shows that the studied modified clays exhibited higher d-value increase with respect to the purified Mts, and the reflection peaks 2θ (°) of plane (001) were displaced towards lower values as a consequence of the ionic liquid intercalation process. ATR/FTIR spectra recorded in the spectral zone 4000-600 cm^{-1} indicated the appearance of new peaks and a significant intensity variation between clays in relation to the type of chosen ionic liquid. These vibrational changes are directly connected to the presence of ionic liquids in clays. XRD and ATR/FTIR investigations show a stronger effect of the [$M(CH_2)$ IM^{2+}] [$2I^-$] dicationic ionic liquid on the Mts than the monocationic ionic liquid and the SWy-3 Mt is more sensitive to monocationic and dicationic ionic liquids than K10 and KSF Mts.

Keywords: Montmorillonite, ATR/FTIR spectroscopy, X-ray diffraction, Monocationic and dicationic ionic liquids.

1. Introduction

Montmorillonites (Mts) are clay minerals belonging to the smectite group with 2:1 phyllosilicate, consisting of a tetrahedral sheet sandwiched between two parallel octahedral sheets, of very fine particle size (usually size < 2 μm) [1]. The high cation exchange capacity (CEC) and the large specific surface area allow montmorillonites to be effective in absorbing both organic and inorganic pollutants. Mts have been widely used in industry, agriculture, pollutant absorption, mycotoxins and barrier catalysis in long-term nuclear waste disposal [2].

Ionic liquids (ILs) are a new class of solvents (green solvents), salts that are liquid at room temperature, consisting of organic cations and organic or inorganic anions. Their real industrial advantages are melting properties at temperatures below 100°C, low vapor pressure, high thermal stability, good solvents for many organic, inorganic compounds in addition to possessing high electrical conductivity, and the possibility to modify or change their properties according to the type of cation or anion [3-5]. Imidazolium and pyridinium are organic cations, and mainly Cl^-, Br^-, I^-, BF_4^-, PF_6^-, and $CF_3SO_3^-$ are the most commonly used [6].

Research on organically modified montmorillonite molecules plays an important role in the intercalation processes. The use of ionic liquids in Mt modification has gained attention due to the fact that the ionic exchange with these compounds enables easy organic modification of mineral clay. Certainly, the presence of ILs organic cations in the Mt structure increases the hydrophobicity of the mineral clay and makes them suitable for absorbing organic substances as pollutants [7-8]. The mechanisms of interactions between ILs and clays and the interlayer configurations of ILs are still undergoing certain debate [9-10]. Previous results from molecular simulation has revealed the presence of interlayer water accompanying the intercalation of ILs and has proved that the chain length of organic cations plays a critical role in manipulating the interaction capacity and arrangement in the clay interlayer [11-12].

The goal of this study was to investigate the interlayer configuration of intercalated ILs with different number of cations (one or two) in three different montmorillonites using XRD, ATR/FTIR analyses. In this study, K10, KSF and SWy-3 montmorillonites were modified with two different ionic liquids based on imidazolium with anion I^-: [$EMIM^+$] [I^-] monocationic ionic liquid and [$M(CH_2)$ IM^{2+}] [$2I^-$] dicationic ionic liquid, previously synthesized in our laboratory.

2. Materials and methods

2.1 Montmorillonites

The K10 and KSF montmorillonites were provided by Sigma-Aldrich. SWy-3 Na-rich Montmorillonite was provided by clay minerals (Aurora, USA).

XRD analyses of K10, KSF and SWy-3 montmorillonites without further treatment revealed the presence of various impurities. The samples required prior purification to extract the clay fraction. The clay purification was carried out according to the same experimental method detailed in the article published by Haouzi et al. [13].

2.2 Synthesis of ionic liquids

The synthesis of [M(CH_2) IM^{2+}] [$2I^-$] dicationic ionic liquid was performed as per Moumene [14]. The synthesis of [$EMIM^+$] [I^-] monocationic ionic liquid was performed as per Noack et al. [3].

IL intercalation into MT

5g of Mt and 5g of ionic liquid were mixed in 250 mL of distilled water solution and shaken on a horizontal mechanical shaker at 400 rpm for 24 hours at room temperature. The mixtures were centrifuged at 5000 rpm for 2 min and the supernatants were passed through 0.45 mm filters before being analyzed by XRD, ATR/FTIR instruments.

X-ray diffraction

XRD patterns of the XRD prepared compounds were recorded using either a Bruker D8-Advance Diffractometer with Cu-Kα radiation (λ_1=1.54056 Å, λ_2=1.54439 Å) equipped with a LynxEye detector or a Bruker D8 Diffractometer with Co- K_α radiation (λ_1=1.78897 Å, λ_2=1.79285 Å) equipped with a Vantec detector operating at 40 kV and 40 mA. The powder patterns were refined using the Rietveld method as implemented in the FullProf program [15]. Single crystal diffraction data were collected using a Bruker D8 Venture diffractometer at 293 K using multilayer optics Mo K_α radiation, λ=0.71073 Å. Data collection, cell refinement and data reduction were performed using the APEX2 program suite.

ATR /FTIR Analyses

The measurements were conducted in the Walloon Agricultural Research Center (CRA-W) (Belgium). Fourier Transform mid-infrared -attenuated total reflectance (ATR/FTIR)

measurements were acquired on a Bruker Vertex II-70 RAM II Spectrometer (Bruker Analytical, Madison, WI) equipped with a Golden Gate diamond ATR accessory TM (Specac Ltd, Slough, United Kingdom). ATR/FTIR spectra [4000-600 cm $^{-1}$] were collected with resolution of 1 cm^{-1} by co-adding 64 scans for each spectrum. OPUS 6.0 Software for Windows was used for spectra collection.

3. Results and discussion

3.1 XRD investigations

XRD analyses were performed on the three purified K10, KSF and SWy-3 momtmorillonites and the modified Mts prepared with mono and dicationic ionic liquids in order to investigate whether the exchange of its interlayer sodium cations with these ionic liquids affects or not the basal spacing of Mt. Here, we present X-ray diffraction patterns of purified K10, KSF and SWy- 3 with wide angle (10-70°) in Fig. 1a) and low angle (6-10°) in Fig. 1b). As shown in Table 1, purified K10, KSF and SWy-3 Mts have almost identical crystalline structures. We observed very similar peak values between the three clays with differences that do not exceed 0.6°. However, we noted a significant difference in SWy-3 with a peak at 22.15°. From Figs. 2a), 2b) and 2c) showing X-ray diffraction patterns of purified K10, KSF and SWy-3 and modified by [EMIM^{+}] [I^{-}] and [M(CH_2) IM^{2+}] [2I^{-}], respectively in low angle 5.5-8.5° and Table 2, the modified clays studied, exhibited an increase in d-values with respect to the purified Mts, and the reflection peaks 2θ (°) of plane (001) displaced towards lower values as a consequence of the intercalation process of ionic liquids in the clay in accordance with Bragg's law. Consequently, between purified K10, KSF and SWy-3 and these same clays modified by [EMIM^{+}] [I^{-}] monocationic ionic liquid, we noted an increase of d-values by +1.05 Å for K10, +1.65 Å for KSF and +1.88 Å for SWy-3. With the [M(CH_2) IM^{2+}] [2I^{-}] dicationic ionic liquid, the increase is even more significant in regard to purified Mts: +1.36 Å for K10 and +2.16 Å for SWy-3. These shifts are the obvious signature of the intercalation of the ionic liquids between the montmorillonite layers. The intercalated distances are clearly influenced by the cation charge in the ionic liquid (mono or dicationic). Certainly, d- spacing increased as the average steric size of the cation increased. These results suggest that the swelling of the clay is directly related to the steric size of the intercalated molecule and are consistent with previous studies [8,12,16-18].

3.2 ATR/ FTIR spectra

3.2.1. Comparison between ATR/FTIR spectra of K10, KSF and SWy-3 MTs

FTIR/ATR spectra [4000-600 cm $^{-1}$] of the three purified K10, KSF and SWy-3 MTs are illustrated in Fig. 3a). In relation to the signal at 1000 cm^{-1}, both spectra were normalized. The assignments of the observed modes in this spectral region are listed in Table 3. All reported peak values were identified by the maximum peak height of the non-adjusted spectra. Curve fitting and fitted frequency values labeled* were performed as per Bresson et al. [19]. On the FTIR/ATR spectra (see Fig. 3a), we distinguished three well-defined spectral regions: 3800-2600, 1800-1300 and 1300-600 cm^{-1}. These three spectral regions are respectively illustrated in figures 4a), 4c) and 4e). For the three different montmorillonites, the signal at 1000 cm^{-1} has the highest intensity.

All samples present similar spectra with specific features i.e., relative intensities and IR band positions as described below. Small changes in bands positions were observed especially for SWy-3 Mt (Table 3).

Region 3800–2600 cm^{-1} (O-H stretching region)

In this spectral region characterized by the O-H stretching modes (Fig. 4a), we observed no real vibrational differences between the 3 clays. All spectra were normalized on the peak at 3620 cm^{-1}. Three more or less defined peaks were observed at 3620 cm^{-1}, assigned to O-H stretching mode of inner hydroxyl groups coordinated to octahedral cations at 3405 and 3230 cm^{-1} corresponding to O-H stretching mode of water [1,16,20-22]. We also observed small intensity differences between the three peaks in comparison to montmorillonitic clays. Table 4 presents the three different intensity ratios between the three observed clay components defined by $I_{3405}/I_{3620}=I_{(\nu(O\text{-}H)\ of\ water)}/I_{(\nu(O\text{-}H)\ related\ cations)}$, $I_{3235}/I_{3620}=I_{(\nu(O\text{-}H)\ of\ water)}/I_{(\nu(O\text{-}H)\ related\ cations)}$ and $I_{3405}/I_{3235}= I_{(\nu(O\text{-}H)\ of\ water)}/I_{(\nu(O\text{-}H)\ of\ water)}$. From this table, we note that purified K10 and KSF have similar intensity ratios, whereas purified SWy-3 is distinguished with variations of the ratio of the intensities. However, we noted a valuable difference in the ratio of the intensities for K10 and KSF between I_{3405}/I_{3620} (0.88 value) and I_{3235}/I_{3620} (0.67 value) while they are assigned in the same manner $I_{(\nu(O\text{-}H)\ of\ water)}/I_{(\nu(O\text{-}H)\ related\ cations)}$. This seems to mean that peaks at 3405 and 3235 cm^{-1} are assigned to the O-H stretching mode of different water molecules: perhaps some water molecules are from the clay surface while others are inside or in the bulk of the clay. As SWy-3 montmorillonite differs from the two others by the high rate of Na^+ in its structure, it seems that this Na^+ contribution is the cause of this particular behavior.

Region 1800–1300 cm^{-1}

In this spectral region characterized by the H-O-H bending modes (O-H deformation of water molecules) (Fig. 4c)), we observe real vibrational differences between SWy-3 MT and the other two. Both spectra were normalized on the mode at 1630 cm^{-1}. The peaks at 1424 and 1370 cm^{-1} assigned to δ(OH) vibration are present for K10 and KSF but not for SWy-3 whereas the peaks at 1714, 1700 and 1630 cm^{-1} also assigned to δ(OH) mode appear for all samples (Socrates, 2004). In Table 4, we present the intensity ratio $k = I_{1700}/I_{1630}=I_{(\delta(O\text{-}H))}/I_{(\delta(O\text{-}H) \text{ of water})}$ according to the samples. We remark two phenomena: this intensity ratio is not equal to 1 leading to conclude that the intensity of these two peaks is not the result from the same water molecules and the greater presence of Na^+ in the structure of SWy-3 changes the vibrational behavior of the water molecules at the level of O-H bending mode (k = 0.62 for K10 and KSF against 0.32 for SWy-3).

Region 1300–600 cm^{-1}

In this spectral region characterized by the numerous modes (Fig. 4e), we observe real vibrational differences between all samples. All spectra were normalized on the peak at 1000 cm^{-1}. ATR/FTIR spectra in this spectral region are adjusted by Lorentzian fitting functions. For K10 and SWy-3 Mts, we counted 11 components whereas for KSF Mt we observed 10 components. Seven peaks are affected to Si-O silica stretching mode: 1171, 1118, 1035, 1000, 798, 785 and 700 cm^{-1}. The AlAlOH, AlFeOH and AlMgOH deformations correspond to peaks at 915, 880 and near 840 cm^{-1} respectively [1,20,22]. The peak at 605 cm^{-1} is simultaneously assigned to Al-O-Si deformation and Si-O-Si deformation. The last peak at 1210 cm^{-1} corresponds to δ(O-H) in plane vibration [20,22-23]. We noted the most intense peak at 1000 cm^{-1} change in frequency between the three clays: 1005 cm^{-1} for K10, 993 cm^{-1} for KSF and 988 cm^{-1} for SWy-3, which corresponds to a variation of approximately 15 cm^{-1}. This mode at 1000 cm^{-1} assigned to Si-O stretching is very sensitive to its near environment connected to the structural composition of the clay and can serve as a witness of the type of clay. We observed small differences of intensity between the four peaks indicated at 1035, 1000, 915 and 880 cm^{-1} in comparison to the studied clays. In Table 4, we present four intensity ratios of $\eta_1=I_{1035}/I_{1000}=I_{(\nu(Si\text{-}O) \text{ in plane})}/I_{(\nu(Si\text{-}O))}$, $\eta_2=I_{915}/I_{1000}=I_{(\delta(AlAlOH))}/I_{(\nu(Si\text{-}O))}$, $\eta_3=I_{880}/I_{1000}=I_{(\delta(AlFeOH))}/I_{(\nu(Si\text{-}O))}$ and $\eta_4=I_{840}/I_{1000}=I_{(\delta(AlMgOH))}/I_{(\nu(Si\text{-}O))}$ according to the samples. Yan *et al.* showed that the positions and relative intensities of the 1046 and 1020 cm^{-1} bands are influenced by water content. They proposed that Si-O stretching vibrations, which are responsible for the presence

of these bands, are somehow coupled to the vibrations of interfacial water molecules [24-25]. However, from our studies in the spectral regions 3800-2600 and 1800-1300 cm^{-1}, we have observed that a larger proportion of Na^+ in the SWy-3 Mt structure has a more significant impact on the vibrational modes of water molecules in comparison to the other two clays. This coupling seems to be respected with regard to the variations of η_1 intensity ratio: η_1 passes from 0.81 for K10 to 0.52 for SWy-3. We remark that η_2, η_3 and η_4 intensity ratios increase according to the type of clays (K10, KSF and SWy-3). For these three intensity ratios and for a same sample, $\eta_3 = I_{(\delta(AlFeOH))}/I_{(\nu(Si\text{-}0))}$ is the lowest. It would seem that the difference in molecular weight between Al, Fe and Mg has an impact on these values (Fe having the heaviest molecular weight).

3.2.2 Comparison between ATR/FTIR spectra of monocationic [EMIM⁺] [I⁻] and dicationic [M(CH_2) IM^{2+}] [$2I^-$]

In Fig. 3b), we present the ATR/FTIR spectrum of monocationic [$EMIM^+$] [I^-] and dicationic [M(CH_2) IM^{2+}] [$2I^-$] in the spectral region 3800-600 cm^{-1}. Table 3 presents the ATR/FTIR bands and their assignments. From this table, we count 45 peaks for the monocationic and 55 peaks for the dicationic. The spectrum of the dicationic ionic liquid contains more peaks in the spectral ranges of 3200-3000 and 1700-1300 cm^{-1}.

In Fig. 4b), we focused on the 3200 – 2600 cm^{-1} FTIR spectral region.

Region 3200-2600 cm^{-1}

In this spectral region, we observed modes assigned to the alkyl C-H and N-H stretching regions [14, 26-27]. It is noted that the dicationic spectrum obtained contains more peaks than the monocationic. Compared with the spectral region 1400-1000 cm^{-1}, the intensities of the modes are lower (See Fig.3b). The difference in behavior between mono and dicationic can be explained by the enrichment of the modes directly related to the cation and imidazole increase. We observed numerous changes in the N-H stretching region: the peak at 3133 cm^{-1} for [$EMIM^+$] [I^-] is divided into halves at 3144 and 3126 cm^{-1} for [M(CH_2) IM^{2+}] [$2I^-$]. We noted the same phenomenon for the peak at 3052 cm^{-1} which is transformed into two peaks at 3066 and 3049 cm^{-1} for [M(CH_2) IM^{2+}] [$2I^-$]. We can conclude that this spectral region is also privileged in differentiating between mono and dicationic ionic liquids.

Region 1800 – 1300 cm^{-1}

In this spectral region (Fig. 4d)), we observed the most changes in two spectral regions: 1700-1600 cm^{-1} assigned to Ring *ν*(C=C) and *ν*(N=C-N) modes and 1600-1500 cm^{-1} assigned to Ring in-plane symmetric/anti-symmetric stretch CH_2(N) and CH_3(N)CN stretch modes [14]. Certainly, we note two phenomena: a duplication of peaks and wavenumber shift. For [EMIM$^+$] [I$^-$], there is a peak at 1698 cm^{-1} which is transformed into two peaks at 1685 and 1668 cm^{-1} for [M(CH_2) IM^{2+}] [2I$^-$]. The same applies to the peak at 1625 cm^{-1}, divided into halves at 1617 and 1606 cm^{-1}.

Similarly, the mode behavior at 1546 cm^{-1} differs greatly between mono and dicationic. In the first, a peak is observed at 1546 cm^{-1} while in the second 2 peaks are observed at 1558 and 1543 cm^{-1}. These bands are assigned to ring in-plane symmetric/anti-symmetric stretching CH_2(N) and CH_3(N)CN stretching. The bond CH_2(N) has greater movement freedom in the [EMIM$^+$] cation (connected with the CH_3-CH_2 (N)). In the [M(CH_2)IM^{2+}] cation, this bond between both cations (N-CH_2-N) is of greater constraint enabling the appearance of new modes at 1558 and 1543 cm^{-1}. Moreover, we noted some wavenumber shifts by observing value increase or decrease: we noted a peak at 1569 cm^{-1} for [EMIM$^+$] [I$^-$] whereas for [M(CH_2) IM^{2+}] [2I$^-$] it is observed at 1581 cm^{-1} (+12 cm^{-1}). Inversely, the peak at 1647 cm^{-1} appears at 1637 cm^{-1} (-10 cm^{-1}). The Ring *ν*(C=C), *ν*(N=C-N), Ring in-plane symmetric/anti-symmetric stretch CH_2(N) and CH_3(N)CN stretching modes can serve as markers of the change from mono to dicationic forms.

We also observe peak duplication between the mono and dicationic in the 1500-1300 cm^{-1} spectral region. The doublet at 1463 and 1445 cm^{-1} assigned to $\delta_{as}(CH_2)$/ CCH HCH antisymmetric bending mode for [EMIM$^+$] [I$^-$] is reduced to a peak at 1454 cm^{-1} for [M (CH_2) IM^{2+}] [2I$^-$], whereas the peaks at 1421 and 1386 cm^{-1} assigned to CH_2(N)/CH_3(N)CN stretching mode are divided into halves at 1435 and 1412 cm^{-1} and at 1392 and 1382 cm^{-1} respectively [14].

Region 1300-600 cm^{-1}

In this spectral region (Fig. 4f), the most intense modes for both ionic liquids are at 1165 cm^{-} assigned to ring $\nu_{as}(CH_2(N))$ and CH_3(N)CN stretching modes, at 850 and 775 cm^{-1} corresponding to the ring and NC(H) bending modes of the imidaziolum cation and at 617 cm^{-1} assigned to ω(N-H) and CH3(N)CN stretching modes. For [M(CH_2) IM^{2+}] [2I$^-$], the peak at 775 cm^{-1} shifted to 760 cm^{-1} (-15 cm^{-1}) and the peaks at 644 and 617 cm^{-1} to 621 (-23 cm^{-1}) and 607 cm^{-1} (-10 cm^{-1}) respectively. Anion interaction is observed at 702 cm^{-1}. For this mode,

significant wavenumber shifts are noted between mono and dicationic: approximately +26 cm^{-1} [3,14]. All these significant changes find their source in the passage from [$EMIM^+$] [I^-] to [$M(CH_2)$ IM^{2+}] [$2I^-$].

Consequently, we can distinguish several spectral regions that reflect vibrational behavior mainly attributed to the clay mineral contribution and other vibrations linked exclusively to ionic liquids. Certainly, three peaks more or less defined at 3620 cm^{-1}, assigned to O-H stretching of inner hydroxyl groups coordinated to octahedral cations and at 3405 and 3230 cm^{-1} corresponding to O-H stretching of water constitute the signature of montmorillonite vibrational behavior whereas the N-H and C-H stretching regions between 3150 cm^{-1} and2820 cm^{-1} and C=N stretching modes between 1570 cm^{-1} and 1520 cm^{-1} are only active for the studied mono and dicationic ionic liquids

3.2.3. Comparison between ATR/FTIR spectra of K10, KSF, SWy-3 modified by [EMIM$^+$] [I$^-$] and [M(CH$_2$) IM^{2+}] [2I$^-$]

In Figs. 5a), 5c) and 5e) we present the ATR/FTIR spectra of purified K10, KSF, SWy-3 modified by [$EMIM^+$] [I^-] in the spectral regions 4000-2500 cm^{-1}, 1800-1300 cm^{-1} and 1200-600 cm^{-1} respectively whereas we introduce in Figs 5b), 5d) et 5f) the ATR/FTIR spectra of purified K10, KSF, SWy-3 modified by [$M(CH_2)$ IM^{2+}] [$2I^-$] in the same spectral regions. In Table 5, we compute their observed ATR/FTIR bands and their assignments. Compared with the IR spectra of the purified clays (Figs 4a), 4c) and 4e)), we observed numerous changes in three spectral regions. Certainly, we note the appearance of new peaks mainly in the spectral regions 3200-2900 cm^{-1} and 1600-1500 cm^{-1} corresponding to the signature of the modes directly associated with the presence of ionic liquids inside clays. We observed that these changes are more significant in the case of [$M(CH_2)$ IM^{2+}] [$2I^-$]. It would also seem that clays do not react in the same manner to the intrusion of the ionic liquid to the inner side of their structure: the intensity of the new peaks is more intense in the case of SWy-3 Mt.

Region 4000-2500 cm^{-1}

At first, from Figs 4a), 5a) and 5b) in the 4000-3200 cm^{-1} spectral region, no vibrational behavior distinction could be observed between purified clays and clays modified by ionic liquids. However, by comparing Tables 3 and 5, we noted significant shifts for two modes assigned to ν(O-H) of water: 3405 and 3230 cm^{-1}. For K10, we observed a shift of approximately + 5 cm^{-1} for peaks at 3405 and 3230 cm^{-1} with [$EMIM^+$] [I^-] and + 15 cm^{-1} for the peak at 3230 cm^{-1} with [$M(CH_2)$ IM^{2+}] [$2I^-$]. For KSF and SWy-3, the wavenumber shifts are more significant: for KSF + 30 cm^{-1} for the peak at 3405 cm^{-1} with [$EMIM^+$] [I^-] and [$M(CH_2)$ IM^{2+}] [$2I^-$], for SWy-3 +

40 cm^{-1} for the peak at 3405 cm^{-1} with [$EMIM^+$] [I^-] and + 25 cm^{-1} for the peak at 3230 cm^{-1} with [$EMIM^+$] [I^-] and [$M(CH_2)$ IM^{2+}] [$2I^-$]. Accordingly, the presence of ionic liquid inside the montmorillonite structure has a direct and very significant impact on these vibrational modes assigned to ν(O-H) of water. In order to estimate this effect, in Table 6 we present an intensity ratio between the three observed modified clays defined by $\mu_1 = I_{3420}/I_{3625}=I_{(\nu(O\text{-}H) \text{ of water})}/I_{(\nu(O\text{-}H) \text{ related cations})}$. In comparison with the same intensity ratio calculated for purified Mts. We note that, the introduction of a monocationic ionic liquid inside the three clays led to a differentiation of the intensity ratio for each modified clay. This would seem to indicate that [$EMIM^+$] [I^-] influences the ν(O-H) mode of water in the three different clays in a different way and applies an action to this mode, because the intensity ratios differ in relation to the purified Mts: K10 μ_1 passes from 0.88 to 0.98, KSF from 0.88 to 0.81 and SWy-3 from 0.83 to 0.75. The passage from monocationic to dicationic ionic liquid seems to have a significant impact solely on this intensity ratio than on SWy-3 Mt. On the other hand, we noticed very significant shifts in the 3200-2800 cm^{-1} spectral region corresponding to N-H, C-H stretching modes related to the presence of ionic liquids in the mixture. By comparing the results obtained for ionic liquids only (Table 3) and those for modified clays (Table 5), we note that the peak at 3133 cm^{-1} assigned to the ν(N-H) mode for [$EMIM^+$] [I^-] shifted to 3161 cm^{-1} for K10 modified by [$EMIM^+$] [I^-] ionic liquid (approximately +30 cm^{-1}). The shift is even more notable for the peak at 3052 cm^{-1} assigned to ν(N-H) and ν(=C-H) modes: approximately +55 cm^{-1}. For KSF, we observed the same phenomenon in the same proportion whereas for SWy-3 modified by [$EMIM^+$] [I^-] the increase is less for both peaks: + 20 and +40 cm^{-1} respectively. As in the case of [$M(CH_2)$ IM^{2+}] [$2I^-$], the introduction of this dicationic ionic liquid inside the clay enables the appearance of new peaks in this spectral region: for modified K10 and KSF the peak at 3162 cm^{-1} is transformed into two peaks at 3165 and 3144 cm^{-1} whereas for modified SWy-3 the peak at 3092 cm^{-1} is divided into three peaks at 3101, 3069 and 3049 cm^{-1}. Similarly to the aforementioned, we can estimate a new intensity ratio between the three observed modified clays defined by $\mu_2 = I_{3160}/I_{3115}=I_{\nu(N\text{-}H)}/I_{[\nu(N\text{-}H),\ \nu(=C\text{-}H)]}$. In contrast to the case of μ_1, modified K10 and KSF have approximately the same behavior for μ_2 with a slight reduction for this intensity ratio with the use of dicationic ionic liquid. On the other hand, modified SWy-3 Mt seems to have the same behavior between μ_1 and μ_2. This phenomenon seems to confirm the specific role played by this clay linked certainly to the significant presence of Na^+ in the SWy-3 structure.

Region 1800–1300 cm^{-1}

In Figs 4c), 5c) and 5d) in the spectral region 1800-1300 cm^{-1}, we again observed specific vibrational behavior for modified SWy-3 Mt compared to modified K10 and KSF Mts. We noticed differences in peak intensities between SWy-3 and two other clays. In comparison with the purified K10, KSF and SWy-3, we observed the existence of new peaks assigned only to the ionic liquid near 1584, 1469, 1450, 1390 and 1328 cm^{-1}, corresponding to CH_2(N)/CH_3(N)CN stretching modes. When the Mts are modified by [M(CH_2) IM^{2+}] [2I$^-$] ionic liquid, it is easier to observe these peaks; a new peak of modified K10, KSF, SWy-3 Mts at 1553 cm^{-1} corresponding to the vibration of C=N stretching mode existing in the imidazolium structure, a significant increase in intensity of two peaks at 1710 and 1326 cm^{-1} assigned respectively to δ(O-H) and the ring in-plane bending modes. These last two phenomena reflect the significant impact of the dicationic ionic liquid on the structure of SWy-3 and on the position of water molecules inside this clay. In order to evaluate the intensity variations of peaks at 1710, 1640 and 1585 cm^{-1}, in Table 7 we introduce different intensity ratios between the three observed modified clays defined by $k_1 = I_{1710}/I_{1640}=I_{\delta(O-H)}/I_{[\delta(O-H) \text{ of water, } \nu(C=N)]}$, $k_2 = I_{1710}/I_{1585}=I_{\delta(O-H)}/I_{\nu(CH2(N))}$ and $k_3 = I_{1640}/I_{1585} = I_{[\delta(O-H) \text{ of water, } \nu(C=N)]}/I_{\nu(CH2(N))}$. In comparison to the values of k for purified K10, KSF and SWy-3 Mts (see Table 4), with the introduction of [EMIM$^+$] [I$^-$] ionic liquid inside these clays, k and k_1 differ significantly: each modified clay has a different value from k_1 as opposed to the case of the purified clay study (modified K10 passes from 0.62 to 0.36, modified KSF from 0.62 to 0.21 and modified SWy-3 from 0.32 to 0.27). When we insert [M(CH_2) IM^{2+}] [2I$^-$] ionic liquid into these clays, we can see a rebalancing between K10 and KSF because they have the same but smaller k_1 value reflecting an increase in the number of rings composed of C=N, and a significant increase for k_1 in the case of SWy- 3 (k_1 passes from 0.32 to 0.84). For the k_2 intensity ratio, we can note the same phenomenon for the three modified Mts. For the k_3 intensity ratio, modified K10 and KSF seem to have the same behavior with an increase in this intensity ratio when we use the dicationic ionic liquid in the clay. For modified Swy-3, we observe the same behavior as k_1 and k_2 with a less significant increase (k_3 passes from 0.41 to 0.64). These results show that in this spectral region, the vibrational behavior of these modes at 1710, 1640 and 1585 cm^{-1} are significant witnesses to the impact of the introduction of the ionic liquid inside the clay.

Region 1300–600 cm^{-1}

From Figs 4e), 5e) and 5f) in the spectral region 1300-1600 cm^{-1}, we observed no real changes between FTIR/ATR spectra of purified Mts and Mts modified by ionic liquids. This is certainly understandable by the fact that in this spectral region, clays and ionic liquids have different but active modes with the same wavenumber.

4. Conclusion

In this study, we characterized by X-ray diffraction and ATR/FTIR spectroscopy, the structural and vibrational changes of purified K10, KSF and SWy-3 Mts and these three clays modified by two ionic liquids [$EMIM^+$] [I^-] and [$M(CH_2)$ IM^{2+}] [$2I^-$].

The XRD studies showed that the clay purification process is validated. K10, KSF and SWy-3 have similar structures with the appearance of a peak at 22.15° solely for SWy-3 Mt. The decrease of the reflection peaks 2θ (°) of plane (001) for the studied modified clays constitutes the signature of the intercalation process of ionic liquids inside clays (Table 8, Table 9, Table 10).

By ATR/FTIR investigation, we showed the specific vibrational behavior of purified and modified SWy-3 through the study of various modes: ν(O-H), ν(=C-H), ν(N-H), rings ν(C=C), rings ν(C=N), ν(CH_2(N)), ν(CH_3(N)) and δ(O-H). By comparison with purified K10, KSF and SWy-3 Mts spectra, we observed the appearance of new peaks in various spectral regions and several variations of intensity in specific modes. To conclude, these studies revealed two significant results: the introduction of ionic liquids into clays has a direct impact on infrared spectra with vibrational markers. In the modified clays studied, certain modes are very sensitive to the passage from [$EMIM^+$] [I^-] to [$M(CH_2)$ IM^{2+}] [$2I^-$] (Table 8, Table 9, Table 10).

Conflicts of interest

There are no conflicts of interest to declare.

Acknowledgment

We would like to thank Quentin Arnould, technician at *Walloon Agricultural Research Centre (CRA-W)*, who participated in the ATR/FTIR measurements.

References

[1] J. Madejova. FTIR techniques in clay mineral studies. Vibrational Spectroscopy, 31 (2003) 1–10.

[2] L.P. Lavikainen, J. T. Tanskanen, T. Schatz, S. Kasa and T. A. Pakknen. Montmorillonite interlayer surface chemistry: effect of magnesium ion substitution on cation adsorption. Theoretical Chemistry Accounts, 134 (2015) 1–7.

[3] K. Noack, P.S. Schulz, N. Paape, J. Kiefer, P. Wasserscheid and A. Leipertz The role of the C2 position in interionic interactions of imidazolium based ionic liquids: a vibrational and NMR spectroscopy study. Physical Chemistry Chemical Physics, 12 (2010) 14153-14161.

[4] H.-C. Kan, M.-C. Tseng and Y.-H. Chu. Bicyclic imidazolium-based ionic liquids: synthesis and characterization. Tetrahedron, 63 (7) (2007) 1644–1653.

[5] E. Srasra, F. Bergaya, J.J. Fripiat. Infrared spectroscopy study of tetrahedral and octahedral substitutions in an interstratified illite-smectite clay. Clays and Clay minerals, 42 (3) (1994) 237-241.

[6] M.I. Kim, D.K Kim, K. V. Bineesh, D.W. Kim, M. Selvaraj and D.W Park. Catalytic performance of montmorillonite clay ion-exchanged with ionic liquids in the cycloaddition of carbon dioxide to allyl glycidyl ether. Catalysis Today, 200 (2013) 24– 29.

[7] D.F. Montano, H. Casanova, W. I. Cardona, L.F. Giraldo. Functionalization of montmorillonite with ionic liquids based on 1-alkyl-3-methylimidazolium: Effect of anion and length chain. Material Chemistry and Physics, 198 (2017) 386-392.

[8] J.A. Fiscal-Ladino, M. Obando-Ceballos, M. Rosero-Moreano, D.F. Montano, W. Cardona, L.F. Giraldo, P. Ritcher. Ionic liquids intercalated in montmorillonite as the sorptive phase for the extraction of low-polarity organic compounds from water by rotating-disk sorptive extraction. Anal. Chim. Acta, 953 (2017) 23-31.

[9] S. Studzinska, M. Sprynskyy, B. Buszewski. Study of sorption kinetics of some ionic liquids on different soil types. Chemosphere, 71 (2008) 2121-2128.

[10] C. Takahashi, T. Shirai, Y. Hayashi, M. Fuji. Study of intercalation compounds using ionic liquids into montmorillonite and their thermal stability. Solid State Ionics, 241 (2013) 53-61.

[11] L. Wu, L. Liao, G. Lv, F. Qin, Z. Li. Microstructure and process of intercalation of imidazolium ionic liquids into montmorillonite. Chemical Engineering Journal, 236 (2014) 306 – 313.

[12] L. Wu, C. Yang, L. Mei, F. Qin, L. Liao, G. Lv. Microstructure of different chain length ionic liquids intercalated into montmorillonite: A molecular dynamics study. Applied Clay Science, 99 (2014) 266-274.

[13] A. Haouzi, M. Kharroubi, El H. Belarbi, S. Devautour-Vinot, F. Henn, J.C. Giuntini. Activation energy for dc conductivity in dehydrated alkali metal-exchanged montmorillonites: experimental results and model. Applied Clay Science, 27 (2004) 67 – 74.

[14] T. Moumene, El H., Belarbi, B. Haddad, D. Villemin, O. Abbas, B. Khelifa, S. Bresson. Vibrational spectroscopic study of ionic liquids: comparison between monocationic and dicationic imidazolium ionic liquids. Journal of Molecular Structure, 1065-1066 (2014) 86-92.

[15] J. Rodriguez-Carvajal. Recent advances in magnetic structure determination by neutron powder diffraction. Physica B condensed matter, 192 (1-2) (1993) 55-69.

[16] R. Plesa Chicinas, H. Bedelean, R. Stefan, A. Maicaneanu. Ability of a montmorillonitic clay to interact with cationic and anionic dyes in aqueous solutions. Journal of Molecular Structure, 1154 (2018) 187-195.

[17] L. Reinert, K. Batouche, J-M. Leveque, F. Muller, J-M. Beny, B. Kebabi, L. Duclaux. Adsorption of imidazolium and pyridinium ionic liquids onto montmorillonite: Characterisation and thermodynamic calculations. Chemical Engineering Journal, 209 (2012) 13-19.

[18] Z. Li, W-T Jiang, P-H Chang, G. Lv, S. Xu. Modification of a Ca-montmorillonite with ionic liquids and its application for chromate removal. Journal of Hazardous Materials, 270 (2014) 169-175.

[19] S. Bresson, M. El Marssi, B. Khelifa . Raman spectroscopy investigation of various saturated monoacid triglycerides. Chem Phys Lipids., 134, (2005) 119-129 22.

[20] J. Madejova and P. Komadel Baseline studies of the clay minerals society source clays: infrared methods. Clays and clay minerals, 49 (5) (2001) 410-432.

[21] C. T. Johnston and G. S. Premachandra. Polarized ATR-FTIR study of smectite in aqueuous suspension. Langmuir, 17 (2001) 3712-3718.

[22] W.P. Gates, J.T. Kloprogge, J. Madejova and F. Bergaya. Infrared and Raman spectroscopies of clay minerals. Developpments in Clay (2017) Science 8. Elsevier.

[23] G. Socrates Infrared and Raman characteristic group frequencies: tables and charts. (2004). John Wiley & Sons.

[24] L. Yan, C.B. Roth, P.F. Low. Changes in the Si−O Vibrations of Smectite Layers Accompanying the Sorption of Interlayer Water. Langmuir, 12 (18) (1996) 4421-4429.

[25] L. Yan, J.W. Stucki Effects of Structural Fe Oxidation State on the Coupling of Interlayer Water and Structural Si−O Stretching Vibrations in Montmorillonite. Langmuir, 15 (13) (1999) 4648-4657.

[26] T. Moumene, El H. Belarbi, B. Haddad, D. Villemin, O. Abbas, B. Khelifa, S. Bresson. Study of imidazolium dicationic ionic liquids by Raman and FTIR spectroscopies: the effect of the nature of the anion. Journal of Molecular Structure, 1083 (2015) 179-186.

[27] T. Moumene, El H. Belarbi, B. Haddad, D. Villmin, O. Abbas, B. Khelifa, S. Bresson. Vibrational spectroscopic study of imidazolium dicationic ionic liquids: the effect of the cation alkyl chain length. Journal of Applied spectroscopy, 83 (2) (2016). 180-186.

Highlights

- The K10, KSF and SWy-3 montmorillonites have similar structures.
- Certain modes are very sensitive to the passage from $[EMIM^{+}][I^{-}]$ to $[M(CH_2)IM^{2+}][2I^{-}]$ for studied modified clays.
- The introduction of ionic liquids into clays has a direct impact on their structures.
- The SWy-3 Mt is more sensitive to the passage from $[EMIM^{+}][I^{-}]$ to $[M(CH_2)IM^{2+}][2I^{-}]$ than K10 et KSF MTs.

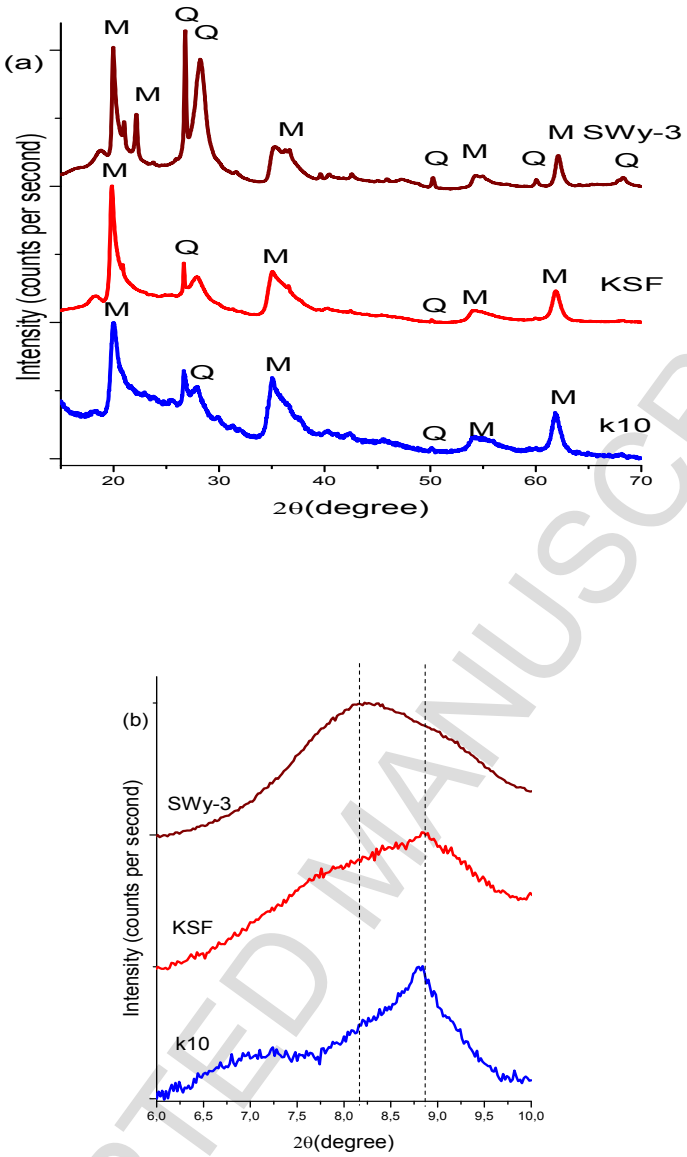

Fig. 1. X-ray diffraction patterns of purified K10, KSF and SWy-3 with (a) broad angles, 10-70° and (b) low angles, 6-10°.

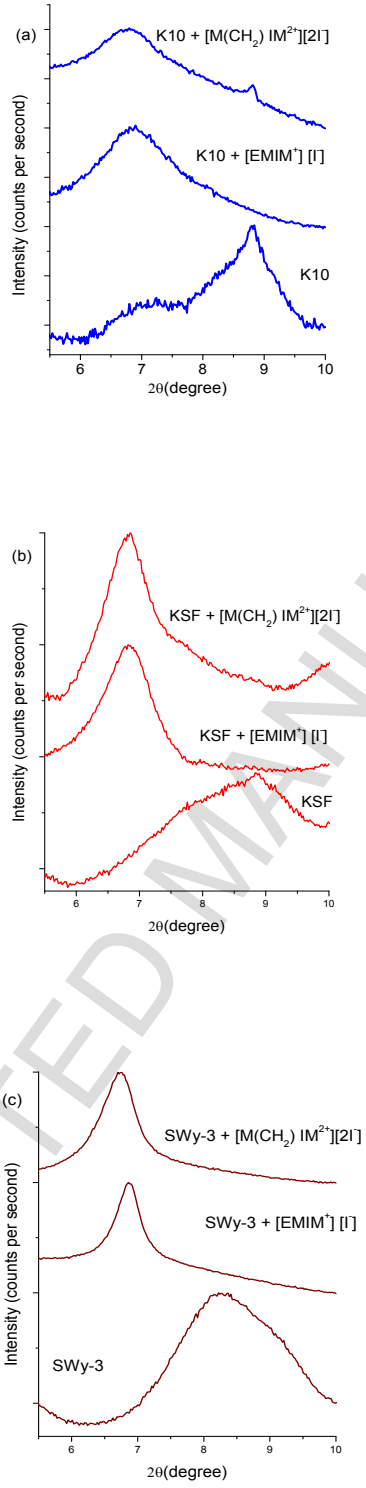

Fig. 2. X-ray diffraction patterns of (a) purified K10, and their modified, (b) pure KSF and their modified and pure SWy-3 and their modified by [EMIM$^+$] [I$^-$] and [M(CH$_2$) IM^{2+}] [2I$^-$] respectively in low angle 5.5-8.5°.

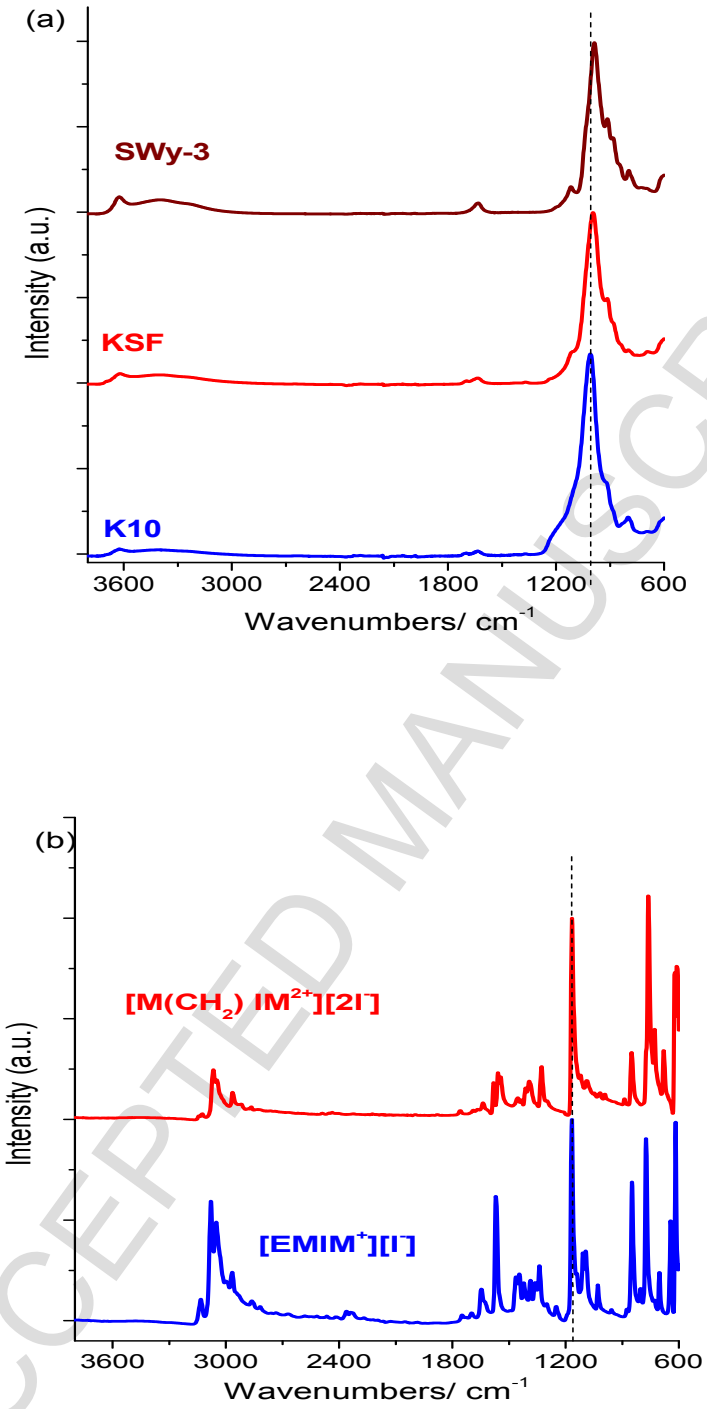

Fig. 3. ATR/IFTR spectra of (a) purified K10, KSF, SWy-3, (b) [EMIM$^+$] [I$^-$], [M (CH_2) IM^{2+}] [2I$^-$] ionic liquids in the spectral range 3700-600 cm^{-1}.

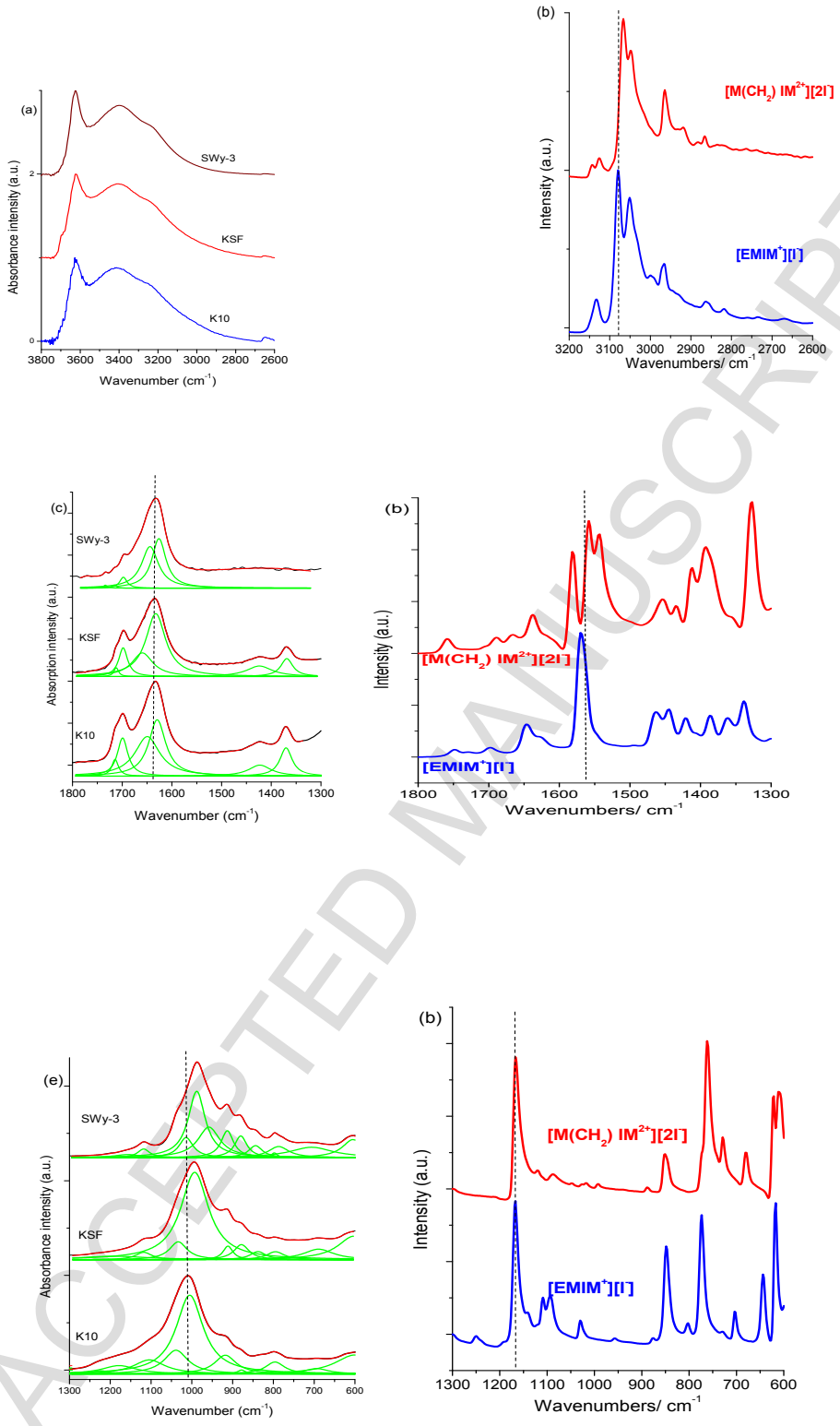

Fig. 4. ATR/IFTR spectra of (a, c and e) purified K10, KSF, SWy-3 montmorillonites and (b, d and f) [EMIM$^+$] [I$^-$], [M(CH$_2$)IM^{2+}][2I$^-$] ionic liquids in the spectral range 3800-2600 cm^{-1}, 1800-1300 cm^{-1} and 1300-600 cm^{-1} respectively.

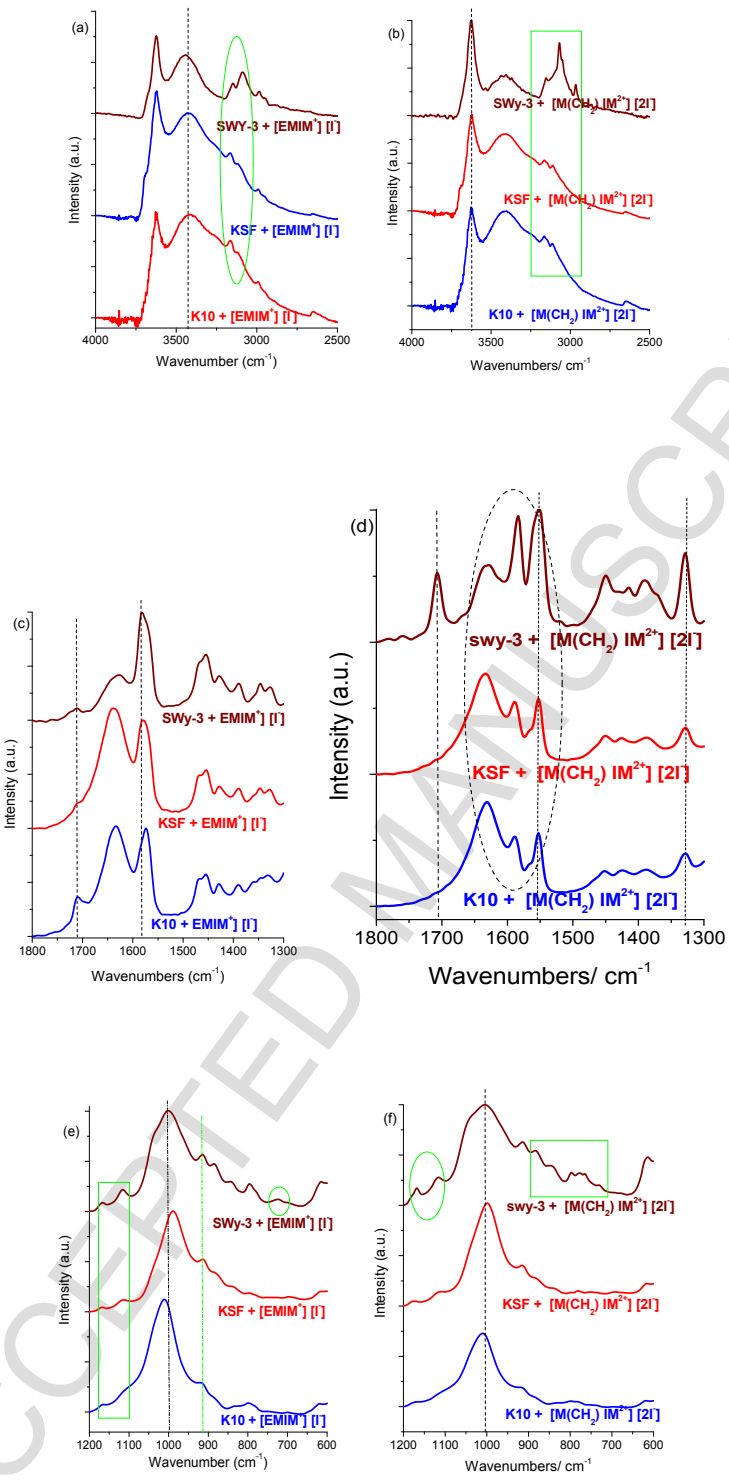

Fig.5. ATR/IFTR spectra of (a, c and e) modified K10, KSF, SWy-3 by [EMIM$^+$] [I$^-$] ionic liquid, the spectra of (b, d and f) modified K10, KSF, SWy-3 by [M(CH$_2$)IM^{2+}][2I$^-$] ionic liquid in the spectral range 3800-2600 cm^{-1}, 1800-1300 cm^{-1} and 1200-600 cm^{-1} respectively.

Table 1.
DRX patterns of purified K10, KSF and SWy-3 Montmorillonites.

K10		KSF		SWy-3		Reference signatures (crystal structure)
2θ (deg)	d (A°)	2θ (deg)	d (A°)	2θ (deg)	d (A°)	
8.15*(sh)	11.74	7.83	11.28	8.04*(sh)	10.95	Montmorillonite
8.82	10.48	8.92	9.90	8.99	9.81	Montmorillonite
18.22	4.86	18.19	4.87	18.81	4.71	Montmorillonite
20.02	4.39	19.82	4.47	19.97	4.44	Montmorillonite
20.93*(sh)	4.26	20.87	4.25	20.99	4.23	Montmorillonite
***	***	***	***	22.15	4.01	Montmorillonite
26.66	3.34	26.66	3.33	26.79	3.33	Quartz
27.90	3.20	***	***	28.19	3.16	Quartz
35.02	2.56	35.26	2.54	35.19	2.55	Montmorillonite
50.18	1.82	50.14	1.82	50.30	1.81	Quartz
54.13	1.69	54.49	1.68	54.22	1.69	Montmorillonite
60.04	1.54	59.96	1.54	60.07	1.54	Quartz
61.85	1.50	61.92	1.50	62.11	1.49	Montmorillonite
***	***	***	***	68.35	1.37	Quartz

Table 2
Comparison of d-space of purified K10, KSF, SWy-3 and their modified obtained from XRD.

Sample name	2θ (deg)	d (A°)
K10	8.15	11.74
K10 + $[EMIM^+][I^-]$	6.90	12.79
K10 + $[M(CH_2)\ IM^{2+}][2I^-]$	6.76	13.10
KSF	7.83	11.28
KSF + $[EMIM^+][I^-]$	6.83	12.93
KSF + $[M(CH_2)\ IM^{2+}][2I^-]$	6.83	12.93
SWy-3	8.04	10.95
SWy-3 + $[EMIM^+][I^-]$	6.88	12.83
SWy-3 + $[M(CH_2)\ IM^{2+}][2I^-]$	6.74	13.11

Table 3:
ATR/IFTR assignments of K10, KSF and SWy-3 montmorillonites and [EMIM$^+$] [I$^-$] and [M(CH_2) IM^{2+}] [2I$^-$] ionic liquids (w = weak; vw = Very weak; m = medium, s = strong; vs = Very strong; * = value of fit; *(sh) = shoulder; ν = Str = stretch; δ = deformation; bend = bending deformation; ω = wagging; s = symmetric; as = antisymmetric; oop = out-of-plane def).

K10	KSF	SWy-3	[EMIM$^+$][I$^-$]	[M(CH_2) IM^{2+}][2I$^-$]	Assignment of	
					K10, KSF and SWy-3	Ionic liquids
4000-2500 cm^{-1}						
3622 (w)	3626(w)	3620 (m)	***	***	*ν*(OH)vibrations of hydroxyl	
3416 (w)	3405(w)	3400 (m)	***	***	*ν*(OH) of water	
3236*(sh)	3231*(sh)	3231*(sh)	***	***	*ν*(OH) of water	
***	***	***	3133(vw)	3144(vw)+3126(vw)		*ν*(N-H)
***	***	***	3078*(sh)	***		*ν*(N-H)
***	***	***	3052 (w)	3066(m)+3049(w)		*ν*(N-H)
***	***	***	3032*(sh)	3044*(sh)+3030 *(sh)		*ν*(N-H), *ν*(=C-H)
***	***	***	2995 (w)	2994*(sh)		*ν*(N-H), *ν*(=C-H)
***	***	***	2967 (w)	2964(w)		*ν*(CH_3(N)HCH),
***	***	***	2938(vw)	2931*(sh)+2917(vw)		ν_{as}(CH_3)
***	***	***	2898*(sh)	2883 (vw)		ν_{as}(CH_2)
***	***	***	2859	2866		ν_{as}(CH_2)
***	***	***	***	2820		ν_s(CH_2)
1800-1300 cm^{-1}						
***	***	1735 (vw)	1750 (vw)	1757 (vw)	δ(H-O-H)	Overtone *ν*(C=C-H)
1714*(sh)	1713*(sh)	1716*(sh)	***	1736-1703*(sh)(vw)	δ(H-O-H)	Overtone *ν*(C=C-H)
1699 (vw)	1698 (vw)	1697 (vw)	1698 (vw)	1685(vw)+1668(vw)	δ(H-O-H)	Ring *ν*(C=C), *ν*(N=C-N),
1650*(sh)	1660*(sh)	1650*(sh)	1647 (w)	1637 (vw)	δ (OH) of water	Ring *ν*(C=C), *ν*(N=C-N),
1630 (w)	1632(w)	1628 (w)	1625 (vw)	1617+1606*(sh)(vw)	δ (OH) of water	Ring *ν*(C=C), *ν*(N=C-N),
***	***	***	1569 (m)	1581 (vw)		ν_{as} (CH_2(N))/ *ν*(CH_3(N)CN)
***	***	***	1546*(sh)(vw)	1558 (vw) + 1543 (w)		*ν* (N=C)
***	***	***	1520 (vw)	1525 *(sh) (vw)		*ν* (C=N)
***	***	***	1463 (w) +1445 (w)	1454 (vw)		δ (CH_2)/ CCH HCH asym bend
1424 (vw)	1424 (vw)	***	1421 (w)	1435 (vw) + 1412 (w)	δ (O-H) ip vibration	CH_2(N)/CH_3(N)CN Str
***	***	***	1386 (w)	1392 (w)+1382*(sh)(w)	δ (O-H) ip vibration	CH_2(N)/CH_3(N)CN Str
1370 (vw)	1369 (vw)	***	***	***	δ (O-H) ip vibration	
***	***		1361 +1338(w)	1350 (w)+1326(m)		Ring ips str/CH_2(N)/ν(CH_3(N)CN)
1300-600 cm^{-1}						
			1299 (vw)+1293*(sh)	1292* (vw)		δ(C-H)
			1250 (vw) + 1235*(sh)	1232 (vw)		δ(C-H)
1209*(sh)	1198*(sh)	***	***	***	δ (O-H) ip vibration	
***	***	***	1166(s)+1159*(sh) (m)	1164(s) +1156*(sh)(s)		Ring ν_{as}(CH_2(N)/CH_3(N)CN Str
1171*(sh)	***	1170*(sh)	***	***	*ν*(Si-O)	
***	***	***	1140 (w)	1133*(sh) (m)	***	ρ(CH_3)
1106*(sh)[5,10]	1118 (m)	1118 (m)[4,10]	1109 (w)	1119 (vw)	*ν*(Si-O)	ν(C-C)
***	***	***	1095*(sh)+1092 (w)	1088 (vw)		ν(C-C)
1035*(sh)	1034*(sh)	1037*(sh)s	1030 (w) + 1023*(sh) (vw)	***	*ν*(Si-O)	CH_3N Str/CH_2N Str
****	***	***	***	1017*(sh)		ν(C-C)
1005 (vs)	993 (vs)	988* (vs)	957 (vw)	993 (vw)	*ν*(Si-O)	ν(C-C)
915 (m)	911 (m)	913 (m)	***	***	δ(Al-Al-OH)	
881*(sh)	879 (m)	880 (m)	877(w)	889 (w)	δ(AlFeOH)	ρ(CH_2)
831*(sh)	838*(sh)	844 (m)[4]	850* (m)+845*(m)	852*(w) + 845*(w)	δ(AlMgOH)	ω(CH_2)
798 (m)	795 (m)	798 (m)	802 (w)	792*(sh)	*ν*(Si-O)	NC(H)N bend/CCH bend
***	***	785 (sh)	***	***	*ν*(Si-O)	
***	***	***	775(s)	774*(sh) +760 (s)		δ(HCCH)/ Ring HCCH asym bend
***	***	***	735*(sh)	741*(sh)		CH_3(N)/ CH_2(N) bend
693*(vw)	690*(w)	704* (vw)	702(w)	728 (m)	*ν*(Si-O)	anion interaction
***	***	***	***	680 (w)		ω(C–H) +ω(N–H)
***	***	***	658 *(sh)	653 (vw)		ω(N-H)/CH3(N)CN Str
***	***	***	644 (m)	621 (m)		ω(N-H)/CH3(N)CN Str
605 (m)	605 (m)	605 (m)	617 (s)	607 (s)	Al-O, Si-O out of plane	ω(N-H)/CH3(N)CN Str

Table 4. Reports of intensity of many peaks of purified K10, KSF and SWy-3 MTS in the spectral range 4000-600 cm^{-1}.

Clays	I_{3405}/I_{3620}	I_{3235}/I_{3620}	I_{3405}/I_{3235}	I_{1700}/I_{1630}	I_{1035}/I_{1000}	I_{915}/I_{1000}	I_{880}/I_{1000}	I_{840}/I_{1000}
K10	0.88± 0.02	0.67± 0.02	1.31± 0.02	0.62± 0.02	0.81± 0.02	0.37± 0.02	0.22± 0.02	0.21± 0.02
KSF	0.88± 0.02	0.67± 0.02	1.31± 0.02	0.62± 0.02	0.66± 0.02	0.50± 0.02	0.37± 0.02	0.41± 0.02
SWy	0.83± 0.02	0.57± 0.02	1.46± 0.02	0.32± 0.02	0.52± 0.02	0.56± 0.02	0.46± 0.02	0.50± 0.02

Table 5

ATR/IFTR assignments of modified K10, KSF and SWy-3 montmorillonites by $EMIM^+$] [I^-] and [$M(CH_2)$ IM^{2+}] [$2I^-$] ionic liquids (w = weak; vw = Very weak; m = medium, s = strong; s = Very strong; * = value of fit; *(sh) = shoulder; *v* = Str = stretch; δ = deformation; bend = bending deformation; ω = wagging; s = symmetric; as = antisymmetric; oop=Out-of-plane def).

K10 + [$EMIM^+$][I^-]	K10+[$M(CH_2)IM^{2+}$][$2I^-$]	KSF + [$EMIM^+$][I^-]	KSF+[M (CH_2)IM^{2+}][$2I^-$]	SWy-3 + [$EMIM^+$][I^-]	SWy-3+[$M(CH_2)$ IM^{2+}][$2I^-$]	Assignment
4000-2500 cm^{-1}						
3648*(sh)	3648*(sh)(w)	3695*(sh)	3648*(sh)	3676 *(sh)	3678*(sh)	*v*(OH)of inner-surface
3626 (w)	3627 (w)	3625(w)	3624 (w)	3626 (w)	3626 (w)	*v*(OH)of inner-surface
3400(w)	3410*(w)	3433 (w)	3427 (w)	3443 (w)	3421 (w)	*v*(OH)of water
3241*(sh)	3251*(sh)	3236*(sh)	3225*(sh)	3259*(sh)	3254 *(sh)	*v*(OH) of water
3161 (vw)	3165 (w)-3142*(sh)	3162 (m)	3165-3144*(sh)	3152(vw)	3157 (w)	*v*(N-H)
3119 (w)	3114 (w)	3117 (w)	3110 (w)	3092 (w)	3101*-3069-3049*	*v*(N-H) and *v*(=C-H)
2989 (vw)	2972*(sh)	2990(w)	2974*(sh)	2988 (vw)	2995 (vw)	*v*(N-H) and *v*(=C-H)
2952*(sh)	***	2953(vw)	***	2949 (vw)	2966 (w)	*v*(CH_3(N)HCH)
1800-1600 cm^{-1}						
1707 (vw)	1694*(sh)	1712 (vw)	1727*(sh)	1711 (vw)	1707 (w)	δ(H-O-H)
1635 (w)	1633 (w)	1643* (w)	1633(w)	1642*-1622	1642 (w)-1626(w)	Ring *v*(C=C), *v*(N=C-N),
1584*(sh)	1589 (w)	1584 (w)	1588(vw)	1584 (m)	1581 (w)	v_{as} (CH_2(N))/ *v*(CH_3(N))
1574 (w)	1566*(sh) -1552(vw)	1576 (w)	1566* -1552	1573*(sh)	1561*(sh)+1552(w)	*v*(C=N)
1470(vw)+1453(vw)	1469*(sh +1452 (vw)	1470-1453	1467*-1450	1469-1452	1470*(sh)+1450(w)	δ (CH_3),
1429 (vw)	1425 (vw)	1424 (vw)	1425 (vw)	1428(vw)	1415 (vw)	δ (O-H) ip vibration
1391(vw)	1388 (vw)	1389 (vw)	1388 (vw)	1389 (vw)	1390 (w)	CH_2(N), CH_3(N) CN str/
***	***	1362-1347	***	1361*-1347(vw)	1369 *(sh)	δ (O-H) ip vibration
1363+1330(vw)	1330 (vw)	1327 (vw)	1329(vw)	1326 (vw)	1328 (w)	ring, *v*(CH_2(N)/CH_3(N))
1300-600 cm^{-1}						
1229*(sh)	1218*(sh)	***	1232*(sh)	1202 *(sh)	***	δ (O-H) ip vibration
1168 (m)	1174 (m)	1169 (m)	1174 (m)	1168(m)	1168 (m)	*v* (CH_2(N)/CH_3(N)CN)
1105*(sh)	1103*(sh)	1116 (m)	1104*(sh)	1117(m)	1119 (m)	*v*(cc), Si-NH-Si Silica
1039*(sh)	1038*(sh)	1037*(sh)	1037*(sh)	1040*(sh)	1048(m)	*v*(Si-O)
1007 (vs)	1006 (vs)	988 (vs)	1006 (vs)	1010* (vs)	1009 (vs)	*v*(Si-O),
914 (m)	914 (m)	913 (m)	913 (m)	914 (s)	913 (m)	δ(Al-Al-OH)
882*(sh)	881*(sh)	878	881*(sh)	882 (s)	880 (m)	δ(AlFeOH)
832 (m)	835*(sh)	836 (m)	832(m)	842 (m)	842 (m)	δ(AlMgOH)
797*(sh)	792*(sh)	792(m)	800-779 (m)	796 m-777*(sh)	798 (m)-777 (m)-763	*v*(Si-O)
***	740*(sh)	744*(sh)	745(m)	727 (m)	730 (m)	*v*(Si-O), anion interaction
696*(sh)	693*(sh)	690 (m)	689*(sh)	690*(sh)	***	*v*(Si-O),
612 (m)	621 (m)	610 (m)	611 (m)	612 (m)	609 (m)	ω(N-H)/CH3(N)CN, Al-O, Si-O oop

Table 6. Reports of intensity of many peaks of modified K10, KSF, SWy-3 by [$EMIM^+$] [I^-] ionic liquid, and by [$M(CH_2)IM^{2+}$][$2I^-$] ionic liquid in the spectral range 4000-2600 cm^{-1}.

Modified Clays	I_{3420}/I_{3625} [$EMIM^+$] [I^-]	I_{3420}/I_{3625} [$M(CH_2)IM^{2+}$][$2I^-$]	Intensity variation	I_{3160}/I_{3115} [$EMIM^+$] [I^-]	I_{3160}/I_{3115} [$M(CH_2)IM^{2+}$][$2I^-$]	Intensity variation
K10	0.98± 0.02	0.95± 0.02	≈	1.17± 0.02	1.11± 0.02	≈
KSF	0.81± 0.02	0.81± 0.02	=	1.20± 0.02	1.13± 0.02	≈
SWy-3	0.75± 0.02	0.42± 0.02	↓↓	0.72± 0.02	0.49± 0.02	↓↓

Table 7. Reports of intensity of many peaks of modified K10, KSF, SWy-3 by [$EMIM^+$] [I^-] ionic liquid, and by [$M(CH_2)IM^{2+}$][$2I^-$] ionic liquid in the spectral range 1800-1300 cm^{-1}.

Clays	I_{1710}/I_{1640} [$EMIM^+$] [I^-]	I_{1710}/I_{1640} [$M(CH_2)IM^{2+}$][$2I^-$]	ΔI	I_{1710}/I_{1585} [$EMIM^+$] [I^-]	I_{1710}/I_{1585} [$M(CH_2)IM^{2+}$][$2I^-$]	ΔI	I_{1640}/I_{1585} [$EMIM^+$] [I^-]	I_{1640}/I_{1585} [$M(CH_2)IM^{2+}$][$2I^-$]	ΔI
K10	0.36± 0.02	0.15± 0.02	↓↓	0.37± 0.02	0.22± 0.02	↓	1.02± 0.02	1.45± 0.02	↑
KSF	0.21± 0.02	0.15± 0.02	↓	0.24± 0.02	0.22± 0.02	↓	1.12± 0.02	1.42± 0.02	↑
SWy	0.27± 0.02	0.84± 0.02	↑↑	0.11± 0.02	0.54± 0.02	↑↑	0.41± 0.02	0.64± 0.02	↑↑

Table 8. Summary of changes in crystal structure and IR functional group band intensity for K10 and K10 modified clays.

XRD results	K10	K10 + [EMIM⁺] [I⁻]	Intensity variations	K10 + [M(CH₂)IM²⁺][2I⁻]	Intensity variations between mono /dicationic
d (A°)	11.74	12.79	↑↑	13.10	↑
IR modes (cm^{-1})	**K10**	**K10 + [EMIM⁺] [I⁻]**	**Intensity variations**	**K10 + [M(CH₂)IM²⁺][2I⁻]**	**Intensity variations between mono /dicationic**
ν(N-H)	no	3161	↑↑	3165	≈
ν(N-H)	no	no		**3142**	↑
ν(N-H)	no	3119	↑	3114	≈
δ(H-O-H)	1700	1707	↑↑	1695	↓↓
$\nu_{as}(CH_2(N))$	no	1584	↑↑	1589	↓
ν(C=N)	no	1574	↑	1566	≈
ν(C=N)	no	no		**1552**	↑↑

Table 9. Summary of changes in crystal structure and IR functional group band intensity for KSF and KSF modified clays.

XRD results	KSF	KSF + [EMIM⁺] [I⁻]	Intensity variations	KSF + [M(CH₂)IM²⁺][2I⁻]	Intensity variations between mono /dicationic
d (A°)	11.28	12.93	↑↑	12.93	≈
IR modes (cm^{-1})	**KSF**	**KSF + [EMIM⁺] [I⁻]**	**Intensity variations**	**KSF + [M(CH₂)IM²⁺][2I⁻]**	**Intensity variations between mono /dicationic**
ν(N-H)	no	3162	↑↑	3165	≈
ν(N-H)	no	no		**3144**	↑
ν(N-H)	no	3117	↑	3110	≈
δ(H-O-H)	1700	1712	↑	1727	≈
$\nu_{as}(CH_2(N))$	no	1584	↑↑	1588	↓
ν(C=N)	no	1576	↑	1566	≈
ν(C=N)	no	no		**1552**	↑↑

Table 10. Summary of changes in crystal structure and IR functional group band intensity for SWy-3 and

SWy-3 modified clays.

XRD results	SWy-3	SWy-3 + [EMIM$^+$] [I$^-$]	Intensity variations	SWy-3 + [M(CH$_2$)IM^{2+}][2I$^-$]	Intensity variations between mono /dicationic
d (A°)	10.95	12.83	↑↑	13.11	↑
IR modes (cm^{-1})	**SWy-3**	**SWy-3 + [EMIM$^+$] [I$^-$]**	**Intensity variations**	**SWy-3 + [M(CH$_2$)IM^{2+}][2I$^-$]**	**Intensity variations between mono /dicationic**
ν(N-H)	no	3152	↑↑	3157	↑
ν(N-H)	no	3092	↑↑	**3101**	↑
ν(N-H)	no	no		**3069**	↑↑↑
ν(N-H)	no	no		**3049**	↑↑
δ(H-O-H)	1700	1711	↑	1707	↑↑↑
ν$_{as}$(CH$_2$(N))	no	1584	↑↑↑	1581	↑
ν(C=N)	no	1573	↑	1561	≈
ν(C=N)	no	no		**1552**	↑↑